

**QME3** Fig. 2. (a) THG intensity  $I_{xy}^{3\omega}$  and  $I_{xx}^{3\omega}$  (open and filled circles) as a function of ellipticity of the incident photons. From this one obtains (b) the phase difference and (c) the amplitude ratio of the underlying independent elements of  $\chi^{(3)}$ .

nonzero components are  $\chi_{xxxx}^{(3)} = \kappa_{xx} e^{i\phi_{xx}}$  and  $\chi_{xyxy}^{(3)} = \kappa_{xy} e^{i\phi_{xy}}$  for the applicable 4/mmm symmetry. As shown in Fig. 2a, we measure the corresponding THG intensities  $I_{xx}^{3\omega}$  and  $I_{xy}^{3\omega}$  as a function of ellipticity of the incident pulses (retardance Δ away from linear polarization). From this, one obtains the phase difference  $\delta = \phi_{xy} - \phi_{xx}$  and amplitude ratio  $\rho = \kappa_{xy}/\kappa_{xx}$ . These values shown in Figs. 2(b,c) exhibit step-like changes concurrent with the appearance of the resonance (Fig. 1). The resonance thus affects differently the products of matrix elements parallel to the same axis,  $\chi_{xxxx}^{(3)}$ , and the mixed products,  $\chi_{xyxy}^{(3)}$ , implying at least a significant contribution of a parity forbidden transition active at  $2\omega$ . Furthermore, it can be shown that  $I_{xx,xy}^{3\omega} = 0$  occurs only for  $\rho = 3$ , a value associated with an overall spherical electronic distribution. As shown in Fig. 2, while  $\rho = 3$  at the resonance, the transition through the resonance is associated with a change of symmetry of the THG tensor. More detailed calculations are underway to link these novel results to the symmetries of the underlying wavefunctions in the  $\text{Sr}_2\text{CuO}_2\text{Cl}_2$  bandstructure.

#### References

1. M.Z. Hasan, et al. Science 288, 1811 (2000).
2. Y.Y. Wang, et al. Phys. Rev. Lett. 77, 1809 (1996).
3. H. Kishida, et al. Nature 405, 929 (2000).

#### QME4 11:00 am

##### Nonlocal effects in the nonlinear optical response of chiral molecules: Third-order nonlinear circular dichroism

H. Mesnil, M. C. Schanne-Klein and F. Hache,  
Optical Bioscience Laboratory Ecole  
Polytechnique F-91128 Palaiseau—France;  
Email: hache@leonardo.polytechnique.fr

Although it was predicted as soon as 1967,<sup>1</sup> third-order nonlinear circular dichroism has never been experimentally observed. In this paper, we investigate this phenomenon in a liquid of chiral molecules. We first perform a theoretical calculation including nonlocal effects in the nonlinear light-matter interaction that allows to get insight into the process and to obtain its order of magnitude.<sup>2</sup> We then demonstrate experimentally the existence of such a third-order nonlinear circular

dichroism with a Ruthenium-tris(bipyridyl) salt that we have under its two enantiomeric (Δ and Λ) forms. Several experiments are carried out with a 1 kHz, 180 fs laser source: a one beam saturation experiment where a saturation of the circular dichroism is clearly observed<sup>3</sup> and a pump-probe experiment. In the latter case, by modulating the polarization of the probe or of the pump from a left to a right circular one, we observe an intensity-dependent circular dichroism (fig. 1). All these experiments are shown to derive from the same nonlinear mechanism, namely a chiral signature in the optical Kerr effect. We furthermore show that our results are in good agreement with our theoretical calculation.<sup>2</sup> Extension of this technique to time-resolved circular dichroism measurement is discussed.

1. S.A. Akhmanov and V.I. Zharikov, JETP Lett. 6, 137 (1967).
2. F. Hache, H. Mesnil and M.C. Schanne-Klein, Phys. Rev. B 60, 6405 (1999).
3. H. Mesnil and F. Hache, Phys. Rev. Lett. 85, 4257 (2000).

#### QME5 11:15 am

##### Frequency-doubling of femtosecond pulses in walk-off compensated N-(4-nitrophenyl)-L-prolinol

Juan P. Torres, Silvia Carrasco and Lluís Torner,  
Lab. of Photonics, Polytechnic Univ. of Catalonia,  
UPC D3, Barcelona 08034, Spain

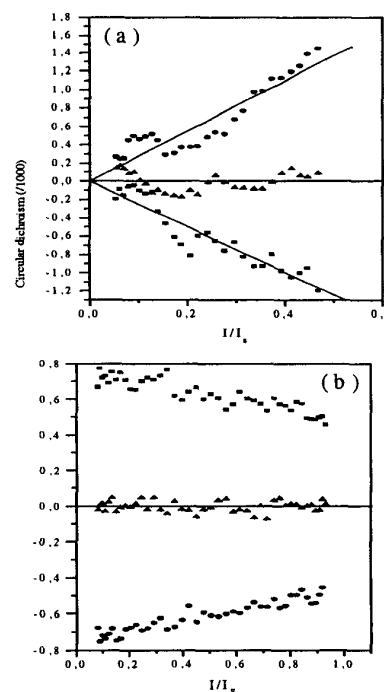
Eric W. VanStryland, CREOL, University of  
Central Florida, Orlando, Florida 32826, USA

N-(4-nitrophenyl)-L-prolinol (NPP) is an organic molecular crystal developed by molecular

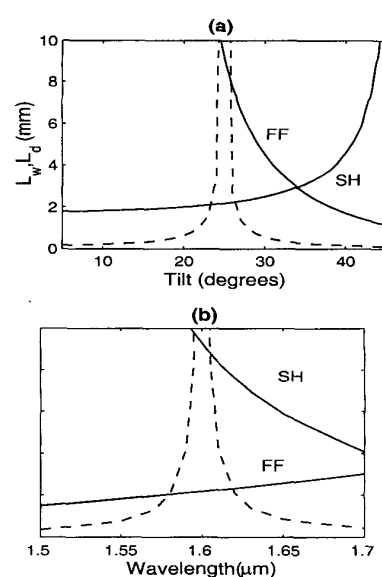
engineering,<sup>1</sup> that exhibits one of the highest phase-matchable second-order susceptibilities reported so far in the near-infrared spectral range ( $d_{\text{eff}} \approx 56 \text{ pm/V}$ ). However, the large spatial and temporal walk-off existing in NPP can limit severely the usefulness of the material away from the noncritical phase-matching (ncpm) wavelength and for shorter pulses.<sup>2</sup>

Here we show that subpicosecond pulses can be efficiently frequency-doubled and mixed in NPP with moderate pump intensities, by employing tilted pulse techniques,<sup>3</sup> which makes use of the large Poynting vector walk-off exhibited by NPP crystals outside the ncpm. Such techniques are based on the diffraction of the input pump wave by a grating so that each spectral component is dispersed in a different direction, thus the resulting signal is a tilted pulse. When the beam width of the incident signal on the grating is large (i.e., a few mm), the effect of diffraction can be accounted for by considering temporal evolution only but with new effective inverse group velocities  $u_v = k'_v + \tan(\psi) \tan(\rho_v)/c$  and group-velocity dispersions  $g_v = k''_v - (\tan(\psi)/c)^2/k_v$ . Here,  $\psi$  is the tilt angle,  $c$  is the velocity of light in vacuum,  $k_v$  are the linear wavenumbers,  $k'_v$  are the inverse group velocities,  $k''_v$  are the group velocity dispersion (GVD) and  $\rho_v$  are the Poynting-vector walk-off angles.

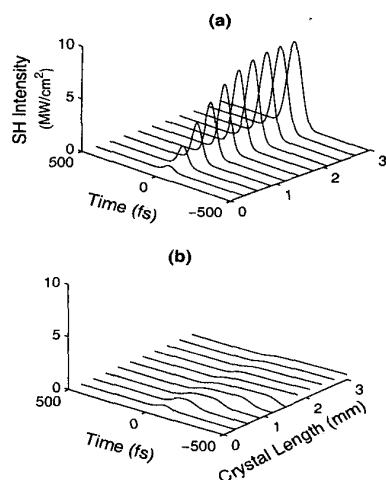
We proceed as follows. First, we calculate the phase-matching angle  $\theta_{pm}$  at the pump wavelength using the appropriate Sellmeier equations. Second, we find the value of the tilt  $\psi_0$  required for group velocity mismatch (GVM) cancellation ( $u_1 = u_2$ ). All this then gives the effective GVDs,  $g_v$ . Figure 1 shows that a tilt-acceptance of several degrees is obtained with walk-off lengths in excess of 5 mm. Similarly, for a fixed tilt a wave-



**QME4** Fig. 1. Pump induced circular dichroism for a polarization-modulated pump (a) or probe (b) vs pump intensity. Squares and dots: Δ and Λ enantiomers, triangles: racemic mixture.



**QME5** Fig. 1. In (a): Effective dispersion lengths,  $L_d$  at the fundamental (FF) and second-harmonic (SH) frequencies (solid lines), and temporal walk-off length,  $L_w$ , (dashed lines), as a function of the tilt angle for a fixed pump wavelength  $\lambda = 1.6 \text{ μm}$ . In (b): Dispersion and walk-off lengths as a function of pump wavelength for a fixed tilt angle  $\psi_0 = 24.9^\circ$ . In both cases:  $\theta = \theta_{pm}$ ,  $\tau = 100 \text{ fs}$  (full width half maximum at intensity).



**QME5** Fig. 2. Detailed evolution of the SH pulse. (a): With GVM compensation; (b): without GVM compensation. Conditions:  $\lambda = 1.6 \mu\text{m}$ ,  $\theta = \theta_{pm}$ ,  $\tau = 100 \text{ fs}$ ,  $I_0 = 10 \text{ MW/cm}^2$  (peak intensity) and  $\omega_0 = 3 \text{ mm}$  (beam waist). No SH pulse at the input.

length bandwidth of several tens of nanometers is obtained. Figure 2 shows the detailed SH pulse evolution whether there is walk-off compensation or not, by solving numerically the evolution equations. The difference is clearly visible: while without walk-off compensation no useful second-harmonic (SH) is generated, a clean, narrow high intensity SH pulse is obtained with the tilted pulse. Losses would reduce the efficiency of frequency doubling in thick crystals, but a high quality output second harmonic pulse is always obtained.

In conclusion, we predict that highly efficient frequency doubling of subpicosecond pulses can be accomplished in walk-off compensated NPP with peak pump intensities in the  $\text{MW/cm}^2$  range, in a wide wavelength band centered around the third telecommunication window. Results are believed to greatly expand the potential applications of NPP to the implementation of parametric devices and cascading phenomena in general.

## References

1. J. Zyss, J.F. Nicoud, and M. Coquillay, *J. Chem. Phys.* **81**, 4160 (1984).
2. Z. Wang et al., *J. Opt. Soc. Am. B* **14**, 76 (1997); G.P. Banfi et al., *Opt. Lett.* **23**, 439 (1998).
3. V.D. Volosov et al., *Sov. J. Quantum Electron.* **4**, 1090 (1975); G. Szabo and Zs. Bor, *Appl. Phys.* **58**, 237 (1994); R. Danielius et al., *Opt. Lett.* **21**, 973 (1996).

## QME6

11:30 am

### Optimization of $\Lambda$ -shaped molecules for second harmonic generation in media with nonpolar alignment

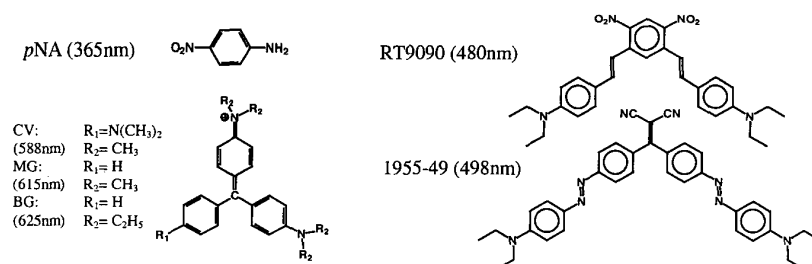
V. Ostroverkhov, R. G. Petschek, K. D. Singer,  
Department of Physics, Case Western Reserve  
University, Cleveland, Ohio, USA;  
Email: vpo@po.cwru.edu

M. He and R. J. Twieg, Department of Chemistry,  
Kent State University, Kent, Ohio, USA

Considerable effort has been directed towards creating organic nonlinear materials for second harmonic generation electro-optic control that would implement the non-vector irreducible components of the first hyperpolarizability tensor.<sup>1,2</sup> In particular, the second-rank tensor component can give rise to macroscopic nonlinearity  $\chi^{(2)}$  in systems having chiral nonpolar symmetry of the bulk, such as  $D_\infty$  or  $D_2$ . These types of alignment can be achieved in uniaxially or biaxially stretched chiral polymers, or in various uniaxial ( $N$ ,  $SmA$ ) and biaxial ( $SmC$ ) liquid crystal phases. To make an efficient frequency conversion material, one has to optimize both the molecular response of the active chromophore and the macroscopic alignment scheme.

The microscopic aspect of the problem is addressed by the quantum mechanical theory of the first hyperpolarizability combined with measurements of the rotationally invariant figures of merit of the relevant irreducible components of

$\beta$ . A technique for determining rotational invariants of  $\beta$  by means of Kleinman disallowed hyper-Rayleigh scattering was designed and reported recently.<sup>3</sup> A quantum mechanical sum-over-states theory of the molecular hyperpolarizability indicated that low-lying states with transition dipole moments perpendicular to the molecule axis (i.e. B-states) are responsible for nonzero Kleinman-disallowed (including the second-rank) part of  $\beta$ . Molecules of  $C_{2v}$  or similar symmetry are common in organic nonlinear optics as they do not have the inversion center (a major requirement for NLO materials), and they also often have a large permanent dipole moment that made them suitable for electric field poled materials. On the other hand, this symmetry allows the existence of electronic states that are odd with respect to two-fold rotation (corresponding to B-representations), which, in turn, results in a second-rank tensor contribution to  $\beta$ . Early studies showed that  $\Lambda$ -shaped chromophores, i.e. those having an electron acceptor (donor) connected to two donor (acceptor) groups with  $\pi$ -conjugated bridges to form a  $\Lambda$  shape, may be of interest as they may have a large second-rank component of  $\beta$  that can be employed in alignment schemes as mentioned above. Here we present systematic measurements of the rotational invariant figures of merit of several  $\Lambda$ -shaped chromophores (Figure 1). Table 1 summarizes the data for the studied materials. One can notice that the figure of merit of the second-rank component for all materials reaches, and in some



**QME6** Fig. 1. Molecular structures and maximum absorption wavelengths of studies materials.

**QME6** Table 1. Rotational invariant for measured  $\Lambda$ -shaped chromophores

Material ( $\lambda$ , nm)		$  \beta_{1ss}  $	$  \beta_{1mm}  $	$  \beta_{2mm}  $	$  \beta_{3ss}  $
(esu $\times 10^{-30}$ )					
pNA (reference)	1560 nm	$7.12 \pm 0.16$	$0.0 \pm 2.1$	$3.0 \pm 2.6$	$4.95 \pm 0.23$
CV		$83.5 \pm 2.1$	$72.2 \pm 2.1$	$84.1 \pm 6.5$	$76.0 \pm 4.2$
MG		$69.8 \pm 1.8$	$14 \pm 30$	$38.6 \pm 9.5$	$54.0 \pm 5.0$
BG		$92.7 \pm 2.1$	$24 \pm 24$	$57.6 \pm 6.1$	$68.0 \pm 3.2$
pNA (reference)	1340	$8.09 \pm 0.09$	$0.0 \pm 2.4$	$3.6 \pm 1.1$	$5.40 \pm 0.19$
RT9090		$266.8 \pm 5.5$	$15 \pm 41$	$128.8 \pm 4.9$	$201.4 \pm 4.6$
1955-49		$316.0 \pm 9.4$	$0 \pm 98$	$180 \pm 35$	$215 \pm 11$
pNA (reference)	1064	$11.2 \pm 1.6$	$4.6 \pm 1.2$	$2.1 \pm 2.6$	$8.2 \pm 1.2$
CV		$305 \pm 58$	$341 \pm 72$	$276 \pm 52$	$398 \pm 81$
pNA (reference)	780 nm	$56.4 \pm 5.9$	$2 \pm 18$	$23.4 \pm 3.8$	$38.3 \pm 4.1$
CV		$552 \pm 42$	$353 \pm 34$	$309 \pm 36$	$287 \pm 31$
MG		$122 \pm 10$	$162 \pm 18$	$120 \pm 13$	$131 \pm 14$
BG		$142 \pm 11$	$186 \pm 16$	$136 \pm 12$	$153 \pm 13$
RT9090		$278 \pm 21$	$112 \pm 27$	$135 \pm 19$	$198 \pm 16$
1955-49		$289 \pm 22$	$119 \pm 25$	$167 \pm 16$	$200 \pm 16$